Doped-CuCl2/Al2O3 catalysts for ethylene oxychlorination: Influence of additives on the nature of active phase and reducibility

(Article begins on next page)

03 February 2025

Doped-CuCl₂/Al₂O₃ catalysts for ethylene oxychlorination: influence of additives on the nature of active phase and reducibility

D. Gianolio, N. B. Muddada, U. Olsbye, and C. Lamberti

Doped-CuCl$_2$/Al$_2$O$_3$ catalysts for ethylene oxychlorination: influence of additives on the nature of active phase and reducibility

D. Gianolio[1]*, N. B. Muddada[2], U. Olsbye[2], and C. Lamberti[1]

[1]Department of Inorganic, Physical and Materials Chemistry, University of Turin, Via P. Giuria 7, 10125 Torino, Italy. Corresponding Author: diego.gianolio@unito.it

[2]inGAP centre of Research-based Innovation, Department of Chemistry, University of Oslo

Abstract

Doped CuCl$_2$/Al$_2$O$_3$ is an industrial catalyst used to produce dichloroethane, key intermediate of the polyvinyl chloride (PVC) chemistry. Using in situ and operando XAS techniques, combined with laboratory techniques, we succeeded in understanding the nature of the active phase and the role played by most used additives for fluid and fixed beds technologies (LiCl, KCl, CsCl, MgCl$_2$, LaCl$_3$). Moreover we were able to quantify relative fraction, reducibility and dispersion of Cu-phases combining different spectroscopic techniques with catalytic tests in a pulse reactor. EXAFS and XANES highlighted that all additives contribute more or less efficiently in increasing the fraction of the active species (supported CuCl$_2$). EXAFS directly, UV-Vis and IR spectroscopies indirectly proved the formation of mixed salts, when KCl or CsCl are added, so displacing the rate determining step from the CuCl oxidation to the CuCl$_2$ reduction. Fully oxidized catalyst is inactive, so copper in the working catalyst, exhibits a I/II mixed valence state. Combining the ethylene conversion, measured with a pulse reactor, with XANES spectra collected after interaction with C$_2$H$_4$, we could differentiate the ability of doped samples to be reduced by ethylene. We obtained slightly different results explainable by the different dispersion of the active phase, measured by CO chemisorption.

1. Introduction

Oxychlorination reaction is largely employed in the modern chemical industry, one of its main application is the production of 1,2-dichloroethane (EDC), a key intermediate in the production of polyvinyl chloride (PVC).[1] Almost all the world production of PVC is based on the polymerization of vinyl chloride monomer (VCM) which, in its turn, is produced by cracking of EDC (1)
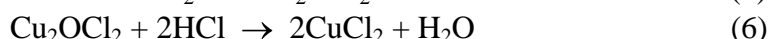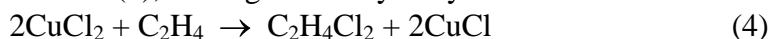
$$C_2H_4Cl_2 \rightarrow C_2H_3Cl + HCl \qquad (1)$$

For the production of EDC, two parallel processes are possible: direct chlorination (2) and oxychlorination (3):

$$C_2H_4 + Cl_2 \rightarrow C_2H_4Cl_2 \qquad (2)$$
$$C_2H_4 + 2HCl + \tfrac{1}{2}O_2 \rightarrow C_2H_4Cl_2 + H_2O \qquad (3)$$

The latter gives two main advantages both from the economic and environmental point of view: it uses cheap and abundant feedstock and it incorporates the recycling of waste hydrogen chloride produced in cracking EDC (1). Thus it reduces consumption of raw materials and exit of useless products in agreement with the modern requests of chemical industry [2; 3; 4]. Oxychlorination reaction (3) is performed at 490-530 K and 5-6 atm. using both air and oxygen in fluid or fixed bed reactors. The catalysts used in industrial reactors are based on CuCl$_2$ supported on γ-alumina with the addition of other chlorides which have the function to improve catalytic performances and suitability for industrial conditions [2; 3; 4; 5; 6; 7; 8]. Typical additives (or dopants) are alkaline or alkaline earth chlorides: KCl is always present in fixed bed technologies, sometimes together with CsCl, NaCl or LiCl [9; 10; 11; 12], while MgCl$_2$ is the most used in fluid bed processes, occasionally in co-presence of LiCl or LaCl$_3$ [13; 14; 15]. After many year of research on the subject, important steps in understanding this complex system have been made, even if only the behavior of base catalyst (containing only CuCl$_2$ without additives) has been mainly discovered. Leofanti et al. [16; 17; 18] have shown that two copper phases are present: an inactive Cu-aluminate where copper ions filled the vacancies of γ-Al$_2$O$_3$, and the active highly dispersed CuCl$_2$ appearing when Cu loading is increased. Further

2

studies:[19; 20; 21] evidenced that the active copper chloride phase follows a three steps redox mechanism: chlorination of ethylene by reduction to CuCl (4); oxidation to an oxychloride (5) and re-chlorination with HCl (6), closing the catalytic cycle.

$$2CuCl_2 + C_2H_4 \rightarrow C_2H_4Cl_2 + 2CuCl \qquad (4)$$
$$2CuCl + \tfrac{1}{2}O_2 \rightarrow Cu_2OCl_2 \qquad (5)$$
$$Cu_2OCl_2 + 2HCl \rightarrow 2CuCl_2 + H_2O \qquad (6)$$

Successively,[21] the $Cu^{II} \leftrightarrow Cu^{I}$ transformation in the base catalyst was monitored with an operando XANES experiment studying the dependence as a function of the temperature and it was found that the rate determining step of the overall process is the CuCl oxidation (5).

In this work we resume the results of an extended analysis to a larger class of doped catalysts ($KCl_3/CuCl_2/\gamma-Al_2O_3$, $MgCl_2/CuCl_2/\gamma-Al_2O_3$, $CsCl/CuCl_2/\gamma-Al_2O_3$, $LiCl/CuCl_2/\gamma-Al_2O_3$, $LaCl_3/CuCl_2/\gamma-Al_2O_3$) [22; 23], where the operando XANES study was coupled with in-situ static XANES/EXAFS on different steps of the reaction mechanism. Catalyst activity in pulse reactor, CO chemisorption, IR and UV-vis spectroscopies also supported x-ray experiments for a full characterization and an improved understanding of the role the additives on the oxychlorination reaction.

2. Synthesis, Experimental and Methods

All samples have been prepared by impregnation of a γ-alumina (Condea Puralox SCCa 30/170, surface area: 168 m^2g^{-1}, pore volume: 0.50 cm^3g^{-1}) with the aqueous solution of the corresponding chlorides following the incipient wetness method as described elsewhere.[16] After impregnation, the samples were dried at 373 K under a dry air flow for 3 hours and then kept at RT. Thin self supported pellets of all catalysts were prepared. Following the nomenclature already used in the previous papers,[16; 17; 18; 19; 20; 21; 24; 25] samples will be labeled according to wt.% content of the different metals (Cu and additive). The amount of copper has been fixed to 5 wt.%, while for the doped samples, an atomic ratio of Cu to dopant metal was equal to 1:1 has been adopted.

The XANES experiments in operando conditions have been performed at the ID24 dispersive EXAFS beamline[26] of the ESRF facility, by feeding a cell containing the sample with a diluted mixture of the three reagents ($C_2H_4 : HCl : O_2 : N_2 = 100 : 36.1 : 7.6 : 180$), representative of the fixed bed process. During the experiment the temperature was increased from 373 to 623 K, kept constant at 623 K for 10 min, and then decreased again to 373 K. In both ramps a speed of 12 K min^{-1} has been adopted, while each XANES spectrum has been obtained by integrating for 30 s resulting in one spectrum each 6 K. The gas output was analyzed by a Balzers Quadstar 422 quadrupole mass spectrometer.

In situ XAS measurements were carried out using synchrotron radiation of the EXAFS13 station at LURE (Orsay, France). Both EXAFS and XANES were measured in transmission mode using air filled ionization chambers. The sampling step was 2.0 and 0.5 eV/point respectively and the integration time was 2 s/point. Extracted $\chi(k)$ have been averaged before the EXAFS data analysis as detailed elsewhere.[27] EXAFS data analysis has been performed using the Arthemis software.[28] For each sample, the averaged $k^3\chi(k)$ function was Fourier transformed in the $\Delta k = 2.0\text{-}13.0$ Å^{-1} interval. For the reduction study, an equilibrium pressure of C_2H_4 of 200 Torr was dosed twice on the catalysts at 500 K for 5 minutes, with an intermediate evacuation. In both in situ and operando set ups the sample was hosted in the ad hoc conceived XAFS cell described elsewhere [29]

3. Results and Discussion

3.1. Determination of the fraction of active copper phase.

The static XAS study was performed on all the catalysts: the undoped $CuCl_2$ supported on γ-alumina and the whole series of doped samples. All samples underwent an activation treatment useful to remove possible extra phases (for example crystalline paratacamite $Cu_2(OH)_3Cl$) and

end up in a configuration were only Cu-aluminate and anhydrous supported $CuCl_2$ are present as shown in previous studies [16; 17; 18; 19; 20].

XANES and EXAFS spectra were acquired and treated separately. Both can give qualitative indications on the differences between the various samples by a visual comparison of the related spectra. It is possible to be more accurate and determine quantitatively the fraction of the different phases present in the samples if a proper reference spectrum for each independent pure phase is available [21; 22; 30; 31; 32; 33]. In our case Cu1.4 sample and anhydrous $CuCl_2$ were used as model compounds of surface Cu-aluminate and of dispersed anhydrous $CuCl_2$ phases, respectively.

XANES spectra, reported in Figure 1a, show a progressive shift from the Cu5.0 spectrum toward the spectrum of anhydrous supported $CuCl_2$ as a function of the dopant used; this suggest an increase of the fraction of $CuCl_2$ active phase and a consequent reduction of the Cu-aluminate with the inclusion of additives. k^3-weighted, Fourier Transform moduli of the EXAFS spectra are reported in Figure 1d; the shape and intensity of the first shell signal show a trend similar to the XANES case. In both cases K3.1Cu5.0 and Cs10.4Cu5.0 curves are more similar to the undoped one, Li0.5Cu5.0 shows an intermediate behavior, while Mg1.9Cu5.0 and La10.9Cu5.0 are closer to the curve related to anhydrous supported $CuCl_2$ phase.

PLEASE INSERT HERE FIGURE 1

For a quantitative analysis, all XANES spectra were simulated by a linear combination of the two spectra corresponding to the pure phases. The only free parameters were the amplitudes factors of the two spectra: x_{al} and x_{Cl}, corresponding to fraction of Cu-aluminate and supported $CuCl_2$ respectively. Despite the two parameters were treated separately and no constrictions were adopted, the sum of the two optimized fractions were always very close to the value expected (100%) and the difference from it was used to estimate the error bars on the results obtained. The complete results are reported in Table 1 (Colum 2, 3) together with the quality of the simulation represented by the R_{factor}. The contribution to the overall XANES signal of the fraction of each phase calculated multiplying the reference spectrum of the pure phase for the corresponding amplitude factor (x_{al} or x_{Cl}) is reported in Figure 1b and 1c, respectively.

In the case of the EXAFS spectra a first shell fit was performed, coordination numbers, Debye-Waller factors and bond length were fixed to the values obtained from the fit of the pure phase spectra. It is possible to easily distinguish the two phases because in the case of Cu-aluminate the first shell is represented by 5 oxygens at a distance of 1.96Å, while in the case of anhydrous $CuCl_2$ the main contribution comes from 4 Cl atoms at a distance of 2.28Å. Only one parameter was free (x_{al}) while the other fraction was fixed so that the sum of the two fraction is 100% (x_{Cl} = 1 - x_{al}). The complete results are reported in Table 1 (Colum 5, 6) together with the R_{factor}, indicator of the good quality of the fits. The single contributions of Cu-O and Cu-Cl paths to the complex first shell EXAFS signal, keeping into account the optimized fraction of the two phases present in the samples, is reported in Figure 1e and 1f, respectively.

PLEASE INSERT HERE TABLE 1

The quantitative analysis of XANES and EXAFS spectra confirmed the behavior suggested from their qualitative observation and the results obtained from the two techniques applied to the same sample are always very similar and have absolute differences lower than 10%. The progression shown by the curves of Cu5.0, K3.1Cu5.0, Cs10.4Cu5.0, Li0.5Cu5.0, Mg1.9Cu5.0, and La10.9Cu5.0 samples, in the following order, results into increasing values of the calculated fraction of supported $CuCl_2$ phase. This behavior is explained considering that, in the case of doped samples, both Cu^{2+} and dopant cations present in the preparation solution compete for the saturation of the surface aluminate phase. If dopant cations have higher chemical affinity for the vacancies, the ratio between the two Cu species will change and the

fraction of the active $CuCl_2$ phase will increase. The dopant cations remaining in solution after saturation of surface cationic vacancies, could precipitate as separate chlorides or form of a mixed salt with $CuCl_2$. The latter case would result into a modification of the chemical nature of active phase and consequently of the catalytic performance. After an accurate observation of the EXAFS second shells signals, combined with UV-vis and IR spectroscopic studies, the formation of K_xCuCl_{2+x} and Cs_xCuCl_{2+x} was found in the case of K- and Cs-additives [23].

3.2. Reducibility of the active copper species by interaction with C_2H_4 and with the reaction feed (C_2H_4, O_2 and HCl) at reaction temperature.

To study the effect of additives on copper reducibility two different approaches were carried out: a static EXAFS/XANES experiment by sending ethylene at 500 K, and an operando XANES experiment by sending the appropriate C_2H_4, O_2 and HCl mixture while progressively changing temperature from 373 to 623 K and down to 373 K.

The results of the operando experiment are reported in Figure 2 for the undoped Cu5.0 sample. A big modification of both the XANES spectrum and its derivative corresponding to a reduction of the sample is clearly visible during heating run, while for all the cooling run an almost stable situation persists meaning that, in presence of reagent flux, the stable form of the active phase is CuCl. To perform a quantitative analysis the spectra of two model compounds for Cu^{II} and Cu^{I} were needed. For each spectrum of the operando experiment it was evaluated the amplitude of the shift at half of the edge jump and the intensity maximum of the derivative then divided by the same values measured between the two references [29]. In this two parallel ways the fraction of Cu^{II} over total copper was evaluated at each moment of the chemical process see bold an solid lines in Figure 2c. The scattered dots represent O_2 conversion, used to measure the activity of the sample, see Eq. (3). O_2 conversion and Cu^{II} reduction start almost together when a cut off temperature, peculiar of each sample, is reached.

PLEASE INSERT HERE FIGURE 2

Repeating the same procedure for each doped sample and the results are reported as insets in Figure 3. Two main groups can be divided depending on their behavior, K3.1Cu5.0 and Cs10.4Cu5.0 start their activity at higher temperatures, firstly they consume O_2 and after 20-50 K also reduction is visible, meaning that the catalysts is already working when the fraction of Cu^{I} is below the XANES detection limit. They don't reach a complete reduction during the heating run and partially reoxidize during the cooling run. Summarizing, for K- and Cs-doped samples, the rate-determining step of the overall oxychlorination reaction is the reduction of the active phase, see Eq. (4). Conversely, Mg1.9Cu5.0 and La10.9Cu5.0 samples, behaves similarly to the undoped one, reaching an almost complete reduction by increasing the temperature and keeping the reduced state in the cooling run. For these samples the rate-determining step of the overall oxychlorination reaction is the oxidation, see Eq. (5). Finally, Cu5.0 and Li0.5Cu5.0 samples seems to represent intermediate cases.

PLEASE INSERT HERE FIGURE 3

The behavior found in the operando experiments (insets in Figure 3) is confirmed by the static XANES spectra acquired after a reduction in ethylene at 500K, reported in the main parts of Figure 3. The scattered curve represents the activated sample, while the colored solid line refer to the sample contacted with C_2H_4 at 500 K. In all frames, also reported as gray dashed line is the spectrum of Cu^{I} model compound. Is it evident that the spectra of K3.1Cu5.0 and Cs10.4Cu5.0 don't show any shift in the edge position because at this temperature their reduction is still not started at 500 K, while the spectra of Cu5.0, Li0.5Cu5.0, Mg1.9Cu5.0 and La10.9Cu5.0 have a lower edge energy with respect of activated ones resulting in a percentage of reduction of 35%, 25%, 50% and 55% respectively. These values were calculated by the edge energy position with

5

the same method adopted for operando experiment. If the fraction of non active Cu-aluminate is considered (see Section 3.1), Cu5.0, Mg1.9Cu5.0 and La10.9Cu5.0 samples show, under the adopted conditions, similar values of reduction of the active phase around 50%. Li0.5Cu5.0 reaches a reduction of about 30% so it is intermediate between the two families of additives. The incomplete reduction of the samples makes more delicate the accurate simulation of the spectra by linear combination of reference spectra as done in the case of the activated catalysts discussed so far. Difficulties came from the simultaneous presence of three different copper phases (Cu-aluminate, $CuCl_2$ and CuCl) and by the fact that CuCl bulk cannot be used as reference spectrum because we are dealing with highly dispersed CuCl nanoparticles[19].

Also the static EXAFS spectra were acquired and confirmed this trend. Both K3.1Cu5.0 and Cs10.4Cu5.0 catalysts are almost unaffected while remaining catalysts exhibit a decrease of the first shell EXAFS signal intensity due to an higher heterogeneity of the first shell Cu-Cl distances in reduced CuCl[34]. As in both phase and amplitude, the Cu-Cl contribution in $CuCl_2$ is almost undistinguishable form that in CuCl, EXAFS fit is not able to discriminate between $CuCl_2$ and CuCl. Consequently, in this specific case, only qualitative information can be extracted from EXAFS.

4. Conclusions

As proved by a previous study, the undoped $CuCl_2/\gamma$-Al_2O_3 catalysts for oxychlorination reaction is formed by two Cu-phases: the inactive Cu-aluminate and the active supported $CuCl_2$ [16]. In the present contribution, we investigated the role played by dopants on the relative fraction and the reducibility of the active phase. A quantitative analysis of EXAFS and XANES of activated samples in static conditions allowed us to prove that all dopants contribute more or less efficiently in increasing the fraction of the active copper species, reaching a value of almost 100% in the case of $MgCl_2$ or $LaCl_3$ additives. The different efficiency is proportional to the ability of the corresponding cations to compete with Cu^{2+} in the occupancy of octahedral surface vacancies of alumina. A qualitative look of the in situ and in operando XANES spectra indicates that addition of $MgCl_2$or $LaCl_3$ does not affect the reducibility of the active $CuCl_2$ phase while KCl and CsCl addition decrease the reducibility because of the formation of mixed salts CuK_xCl_{2+x} and $CuCs_xCl_2$. The behavior of Li-doped sample is intermediate between the two cases.

References

[1] K.S. Go, Y. Kim, S.R. Son, S.D. Kim, Chem. Eng. Sci. 65 (2010) 499.

[2] J.S. Naworski, E.S. Evil. in: B.E. Leach, (Ed.), Applied Industrial Catalysis, Accademic Press, New York, 1983, pp. 239.

[3] M.N. Newmann, Encyclopedia of Polymer Science and Engineering, Wiley, New York, 1985.

[4] M. Garilli, P.L. Fatutto, F. Piga, La Chimica e l'Industria, Milan 80 (1998) 333.

[5] A. Arcoya, A. Cortes, X.L. Seoane, Can. J. Chem. Eng. 60 (1982) 55.

[6] W.D. Mross, Catal. Rev. Sci. Eng. 25 (1983) 591.

[7] X.J. Lu, J. Liu, G.D. Zhou, Y.N. Li, K.J. Xhen, W.X. Li, T.X. Cheng, Chin. J. Catal. 26 (2005) 587.

[8] L. Xueju, L. Jie, Z. Guangdong, Z. Kaiji, L. Wenxing, C. Tiexin, Catal. Lett. 100 (2005) 153.

[9] P.R. Laurer, G. Krome, L. Cordemans, R. Seifert, E. Danz, Euro Pat. 54674 (1981).

[10] K. Shiozaki, A. Onischi, Euro Pat. 62320 (1982).

[11] I. Fatutto, D. Carmello, A. Marsella, Euro Pat. 1053789 (2000).

[12] P.S.S. Prasad, K.B.S. Prasad, P.K. Rao, V.K. Kaushik, J. Mater. Sci. 32 (1997) 1479.

[13] H. Derieth, R. Walter, G. Weidenbach, M. Strebbele, Euro Pat. 255156 (1988).

[14] J.S. Eden, J.A. Cowfer, US Pat. 4849393 (1989).

[15] D. Carmello, M. Grilli, P. Fatutto, L. Caccialupi, Euro Pat. 1045731 (1999).

[16] G. Leofanti, M. Padovan, M. Garilli, D. Carmello, A. Zecchina, G. Spoto, S. Bordiga, G.T. Palomino, C. Lamberti, J. Catal. 189 (2000) 91.

[17] G. Leofanti, M. Padovan, M. Garilli, D. Carmello, G.L. Marra, A. Zecchina, G. Spoto, S. Bordiga, C. Lamberti, J. Catal. 189 (2000) 105.

[18] C. Prestipino, S. Bordiga, C. Lamberti, S. Vidotto, M. Garilli, B. Cremaschi, A. Marsella, G. Leofanti, P. Fisicaro, G. Spoto, A. Zecchina, J. Phys. Chem. B 107 (2003) 5022.

[19] G. Leofanti, A. Marsella, B. Cremaschi, M. Garilli, A. Zecchina, G. Spoto, S. Bordiga, P. Fisicaro, G. Berlier, C. Prestipino, G. Casali, C. Lamberti, J. Catal. 202 (2001) 279.

[20] G. Leofanti, A. Marsella, B. Cremaschi, M. Garilli, A. Zecchina, G. Spoto, S. Bordiga, P. Fisicaro, C. Prestipino, F. Villain, C. Lamberti, J. Catal. 205 (2002) 375.

[21] C. Lamberti, C. Prestipino, F. Bonino, L. Capello, S. Bordiga, G. Spoto, A. Zecchina, S.D. Moreno, B. Cremaschi, M. Garilli, A. Marsella, D. Carmello, S. Vidotto, G. Leofanti, Angew. Chem. -Int. Edit. 41 (2002) 2341.

[22] N.B. Muddada, U. Olsbye, L. Caccialupi, F. Cavani, G. Leofanti, D. Gianolio, S. Bordiga, C. Lamberti, Phys. Chem. Chem. Phys. 12 (2010) In Press.

[23] N.B. Muddada, U. Olsbye, G. Leofanti, D. Gianolio, F. Bonino, S. Bordiga, T. Fuglerud, S. Vidotto, A. Marsella, C. Lamberti, Dalton Trans. 39 (2010) 8437.

[24] C. Lamberti, C. Prestipino, S. Bordiga, G. Berlier, G. Spoto, A. Zecchina, A. Laloni, F. La Manna, F. D'Anca, R. Felici, F. D'Acapito, P. Roy, Nucl. Instrum. Meth. B 200 (2003) 196.

[25] C. Lamberti, S. Bordiga, F. Bonino, C. Prestipino, G. Berlier, L. Capello, F. D'Acapito, F.X. Llabres i Xamena, A. Zecchina, Phys. Chem. Chem. Phys. 5 (2003) 4502.

[26] M. Hagelstein, A. San Miguel, A. Ressler, A. Fontaine, J. Goulon, J. Phys. IV, Paris 7 (1997) C2 303.

[27] C. Lamberti, S. Bordiga, D. Arduino, A. Zecchina, F. Geobaldo, G. Spanò, F. Genoni, G. Petrini, A. Carati, F. Villain, G.J. Vlaic, Phys. Chem. B 102 (1998) 6382.

[28] B. Ravel, M. Newville, J. Synchrot. Radiat. 12 (2005) 537.

[29] C. Lamberti, C. Prestipino, S. Bordiga, G. Berlier, G. Spoto, A. Zecchina, A. Laloni, F. La Manna, F. D'Anca, R. Felici, F. D'Acapito, P. Roy, Nucl. Instrum. Methods Phys. Res. Sect. B-Beam Interact. Mater. Atoms 200 (2003) 196.

[30] C. Prestipino, G. Berlier, F.X. Llabres i Xamena, G. Spoto, S. Bordiga, A. Zecchina, G. Turnes Palomino, T. Yamamoto, C. Lamberti, Chem. Phys. Lett. 363 (2002) 389.

[31] E. Groppo, C. Prestipino, F. Cesano, F. Bonino, S. Bordiga, C. Lamberti, P.C. Thune, J.W. Niemantsverdriet, A. Zecchina, J. Catal. 230 (2005) 98.

[32] R. Le Toquin, W. Paulus, A. Cousson, C. Prestipino, C. Lamberti, J. Am. Chem. Soc. 128 (2006) 13161.

[33] A. Piovano, G. Agostini, A.I. Frenkel, T. Bertier, C. Prestipino, M. Ceretti, W. Paulus, C. Lamberti, J. Phys. Chem. C 115 (2011) 1311.
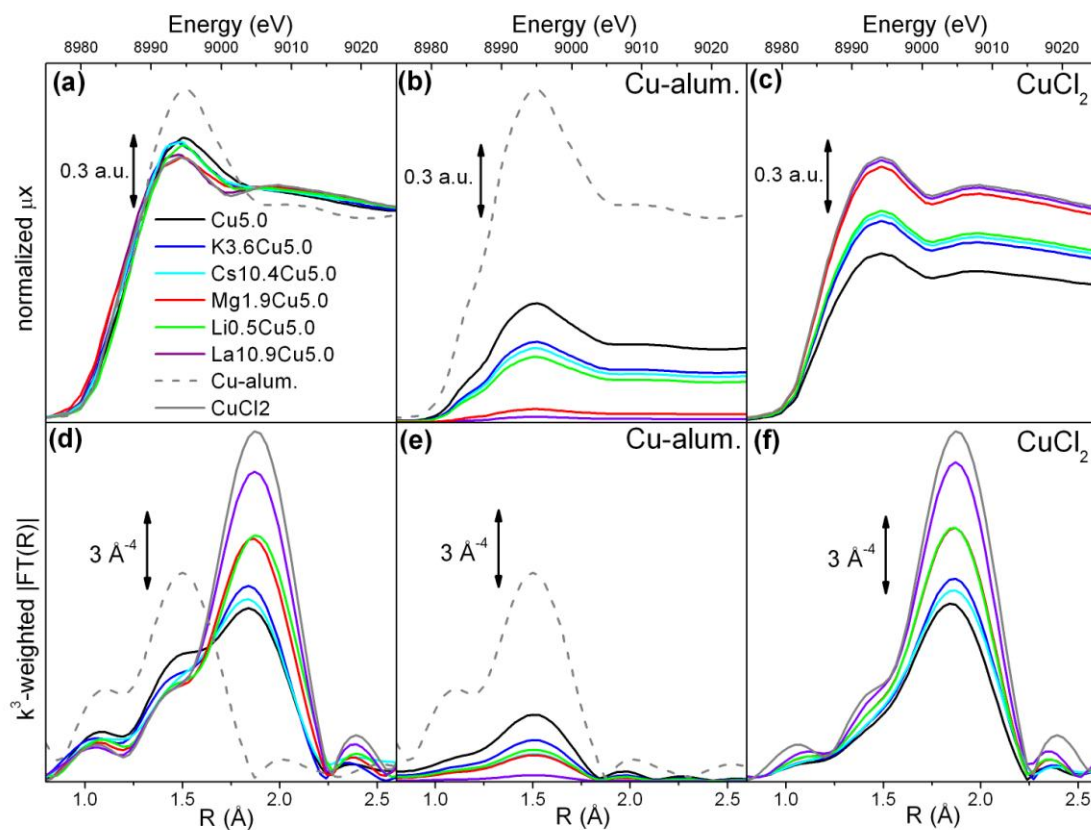
[34] S. Hull, D.A. Keen, Phys. Rev. B 50 (1994) 5868.

Figure 1. Parts (a) and (d) XANES and Moduli of k^3-weigted, phase uncorrected, FT of the EXAFS spectra of all activated samples compared with reference spectra of pure Cu-aluminate phase and pure $CuCl_2$ supported phase. Parts (b), (c), (e) and (f) Contributions to XANES and EXAFS spectra of the fraction of Cu-aluminate and $CuCl_2$ phases present in each sample, the percentages of the two phases were evaluated by a fit of the experimental spectra, numerical values are reported in Table 1.
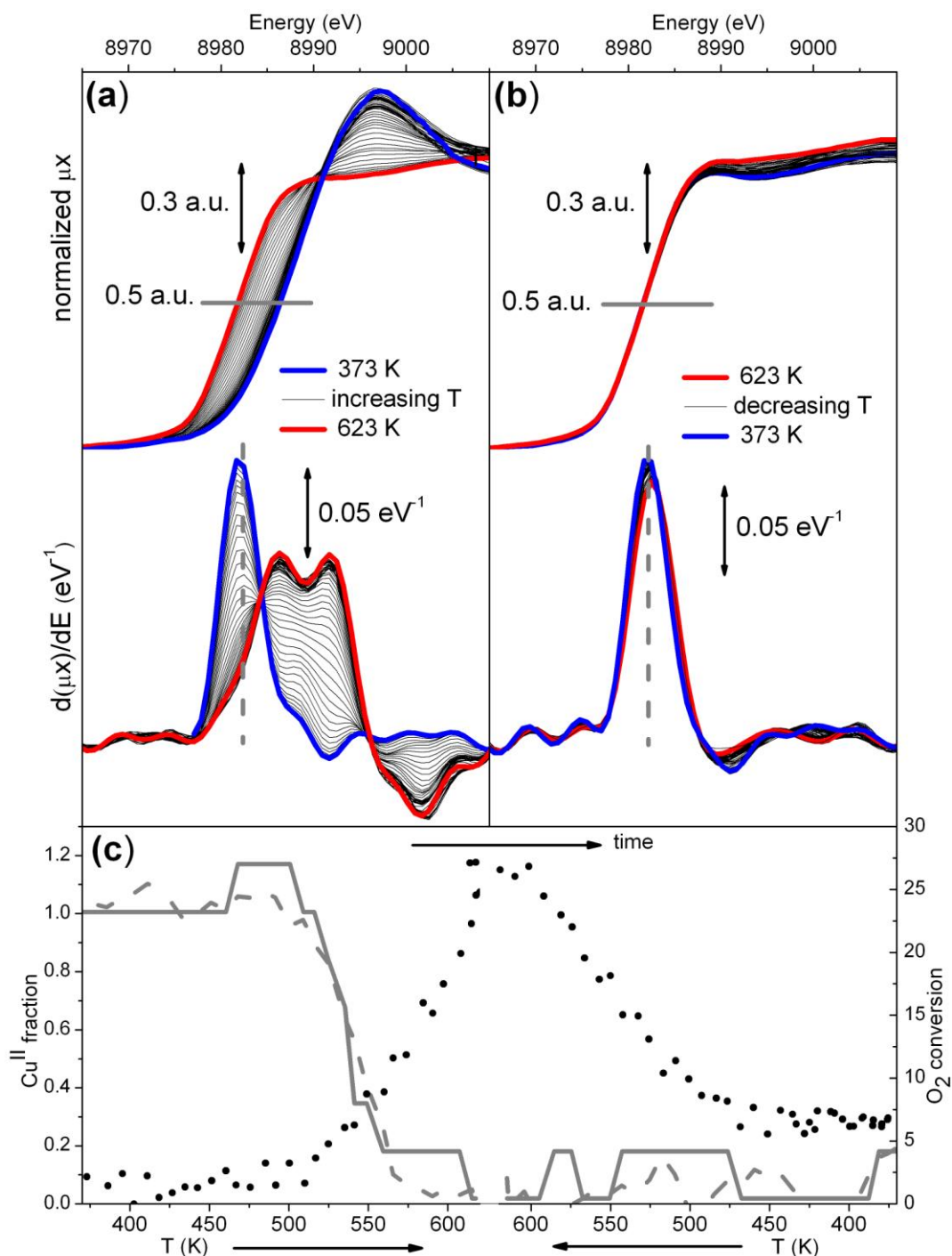
Figure 2. Part (a): operando XANES spectra (top) and corresponding derivative (bottom), acquired by increasing the temperature from 373 to 623 K, Part (b) as part (a) during the cooling step from 623 down to 373 K. Each spectrum corresponds to a step in T of 6 K. In red and blue are evidenced the first and last spectra. Part (c) Fraction of Cu^{II} over total copper evaluated by position of the edge (continuum grey line) and by intensity of the maximum of derivative (dashed grey line), dots indicates the quantity of O_2 converted measured by mass spectrometer.
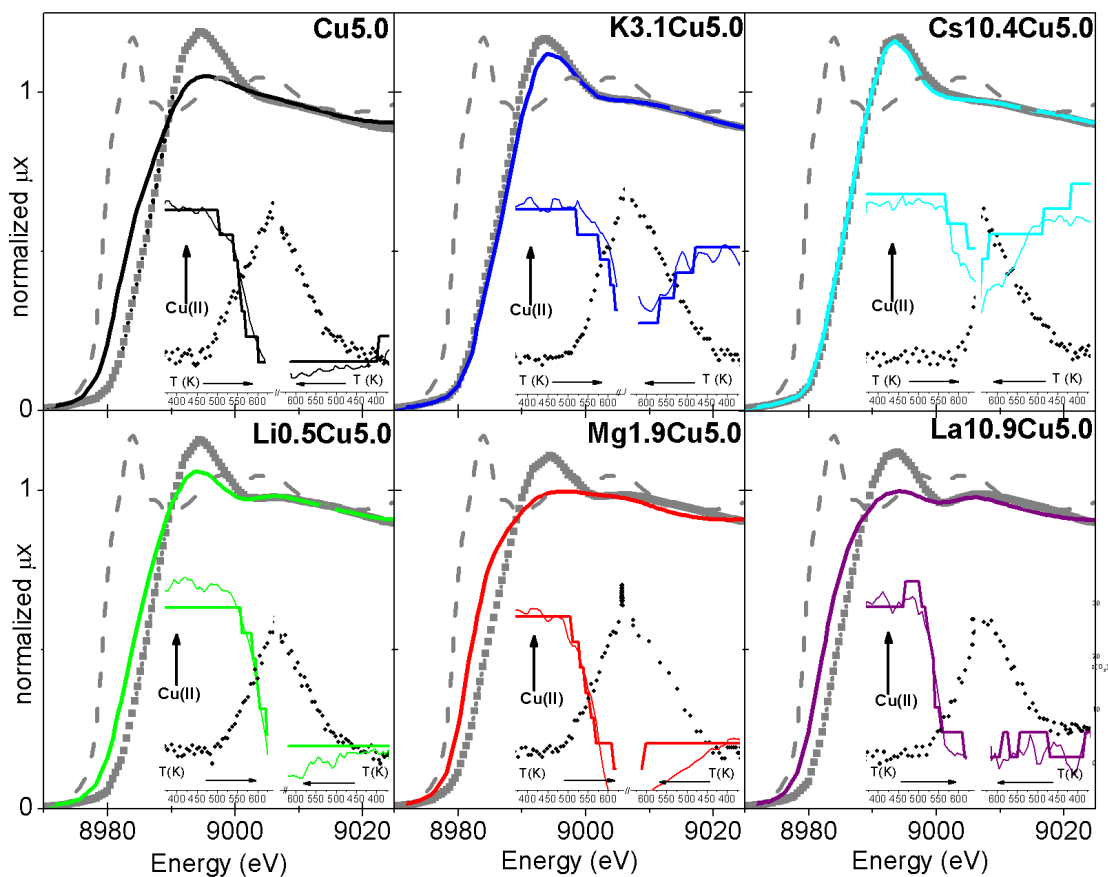
Figure 3. Main parts: XANES static spectra of doped samples before (grey scattered curves) and after (colored solid lines) reduction by ethylene at 500K compared with a spectrum of pure Cu^I chloride (dashed grey line; same curve in all frames). The insets show the results of operando experiments reporting the evolution of the Cu^{II} fraction along the heating and cooling runs estimated from the edge shift (bold colored line) and from the intensity of the maximum of the first derivative (full colored line) together with the catalyst activity (scattered dots).

Table 1. Relative fractions of the Cu-aluminate (x_{al}) and supported $CuCl_2$ (x_{cl}) phases present in the different catalysts and reported in percentage. Columns 2-3: as determined by the linear combination of the XANES spectra of Cu1.4 and $CuCl_2$ model compounds. Columns 5,6: as determined via a standard two-phases Cu-O and Cu-Cl EXAFS fit of the first shell in the 1.0-2.3 Å range, fixing the sum of fractions to unit. Also reported are the indexes of the goodness of the fits $(R_{factor})^2$ for XANES (column 4) and R_{factor} from FEFF code for EXAFS (column 7). Last three columns reports the results of operando XANES experiment, fraction of Cu^{II} at the end of the heating run (623 K) and at the end of the cooling run (373 K), and the temperature of starting of reduction and of oxygen conversion in the heating run.

Samples	XANES linear comb. fit			EXAFS 1st shell fit			Operando XANES		
	100 x_{al}	100 x_{Cl}	$R_{fact}{}^2$	100 x_{al}	100 x_{cl}	R_{FEFF}	%Cu^{II} 623K	%Cu^{II} 373K	T_{red}/T_{O2} (K)
Cu5.0	35.8 ± 0.2	63.8 ± 0.6	0.13	32 ± 3	68 ± 7	0.003	0	0-20	480/480
K3.1Cu5.0	24.2 ± 0.1	75.9 ± 0.4	0.06	20 ± 1	80 ± 5	0.033	35	70	480/520
Cs10.4Cu5.0	22.3 ± 0.2	78.2 ± 0.8	0.05	14 ± 1	86 ± 5	0.038	45	100	560/580
Li0.5Cu5.0	19.7 ± 0.3	79.7 ± 1.0	0.04	15 ± 1	85 ± 5	0.014	25	0-10	500/550
Mg1.9Cu5.0	4.0 ± 0.2	96.4 ± 4.0	0.002	9 ± 1	91 ± 5	0.012	0	10	490/480
La10.9Cu5.0	1.7 ± 0.3	98.9 ± 6.0	0.001	3 ± 0.3	97 ± 8	0.005	0-10	0-10	510/520